DOI: 10.1590/2317-4889201620160031

ARTICLE

Seismic expression of depositional elements associated with a strongly progradational shelf margin: northern Santos Basin, southeastern Brazil

Expressão sísmica de elementos deposicionais associados a uma margem de plataforma fortemente progradante: Eoceno do norte da bacia de Santos, margem sudeste brasileira

Fábio Berton[1]*, Fernando Farias Vesely[1]

ABSTRACT: Seismic facies analysis and seismic geomorphology are important tools for the analysis of depositional elements in subsurface. This paper aimed to investigate the character and genesis of depositional elements and erosive features associated with an Eocene progradational shelf margin in northern Santos Basin. Identified seismic facies are interpreted as shelf-margin deltas/shoreface deposits, tangential (oblique) clinoforms, sigmoidal clinoforms, topset reflectors, mass-transport deposits and turbidites. These facies are grouped into four associations representing periods of relatively constant environmental conditions. Association 1 is composed of shelf-margin deltas/shoreface deposits, tangential clinoforms and extensive sand-rich turbidites disposed as submarine channels and frontal splays. A progressive increase in clinoform angle within this association has been identified, culminating in high-relief sigmoidal clinoforms with less voluminous turbidites of facies association 2. Association 3 is composed by subparallel to divergent topset reflectors, interpreted as continental to shelfal deposits placed during base-level rises. These are always truncated basinward by slump scars, formed as a consequence of sediment overload at the shelf margin during aggradations. Association 4 is composed of sigmoidal clinoforms, mass-transport deposits and turbidites. Early clinoforms are steeper as a consequence of the topography of the slump scars. Subsequently, dip angles become progressively gentler as the system approach to the equilibrium profile. The steep physiography was favorable for canyon incision, which played an important role in turbidite deposition. Mass-transport deposits, formed subsequent to slope collapse, are composed of mud-rich diamictites, and show strong internal deformation.

KEYWORDS: Seismic facies; Seismic geomorphology; Deep-marine deposition; Mass-transport deposits; Turbidite systems.

RESUMO: *A análise de fácies sísmicas e a geomorfologia sísmica são ferramentas importantes para o estudo de elementos deposicionais em subsuperfície. Neste trabalho foram avaliadas as características e a gênese de elementos deposicionais e de feições erosivas associadas a uma margem progradante desenvolvida no Eoceno no norte da bacia de Santos. As fácies sísmicas identificadas são interpretadas como deltas de margem de plataforma/depósitos de shoreface, clinoformas tangenciais (oblíquas), clinoformas sigmoides, depósitos de topset, depósitos de transporte em massa e turbiditos. As fácies foram agrupadas em associações que representam períodos com condições ambientais relativamente constantes. A associação 1 é composta de deltas de margem de plataforma/depósitos de shoreface, clinoformas tangenciais e depósitos turbidíticos arenosos, dispostos em canais submarinos e espraiamentos frontais. Um aumento progressivo no ângulo das clinoformas culmina na formação de clinoformas sigmoides com grandes dimensões verticais e turbiditos que compõem a associação 2. A associação 3 é constituída de refletores subparalelos a divergentes, interpretados como depósitos continentais a plataformais formados durante subidas do nível de base. Esses refletores são truncados em direção à bacia por cicatrizes de escorregamento formadas em consequência da sobrecarga sedimentar na plataforma durante agradações. A associação 4 consiste em clinoformas sigmoides, depósitos de transporte em massa e turbiditos. As clinoformas mais antigas são mais íngremes, em função da topografia imposta pelas cicatrizes de escorregamento. Os ângulos diminuem progressivamente, enquanto o sistema se aproxima do perfil de equilíbrio. Depósitos de transporte em massa, formados após o colapso do talude, são compostos de diamictitos argilosos com intensa deformação interna.*

PALAVRAS-CHAVE: *Fácies sísmicas; Geomorfologia sísmica; Deposição marinha profunda; Depósitos de transporte em massa; Sistemas turbidíticos.*

[1]Department of Geology, Universidade Federal do Paraná – UFPR, Curitiba (PR), Brasil. *E-mail: fabioberton1@yahoo.com.br, vesely@ufpr.br*

*Corresponding author.

Manuscript ID: 20160031. **Received in:** 02/26/2016. **Approved in:** 10/10/2016.

INTRODUCTION

The Eocene interval in northern Santos basin, Brazilian offshore, comprises a complex of high-relief progradational clinoforms (Moreira *et al.*, 2001; Henriksen *et al.* 2011; Dixon, 2013; Berton & Vesely, 2016) associated with shelf-margin accretion developed under relatively high-sediment supply and low accommodation rates. Because of these characteristics, depositional elements from outer shelf to basinal settings are well preserved, including slope clinoforms, submarine channels and lobes, slump scars and mass-transport deposits (e.g., Moreira & Carminatti, 2004). The succession is well imaged by two- and three-dimensional seismic surveys on oil exploration, providing the opportunity of investigating the depositional architecture by applying concepts and methods of seismic facies analysis and seismic geomorphology.

Seismic facies analysis and seismic geomorphology (e.g., Posamentier & Kolla, 2003) are important tools for seismic stratigraphy and hydrocarbon exploration, allowing a detailed visualization of internal and external architecture of depositional elements in subsurface, and have been specially applied to infer sedimentary processes operating in deep-marine environments (e.g., Benan & Cauquil, 2000; Prather & Steele, 2000). Despite the indirect character of seismic data and inherent difficulties associated to limited data resolution (see Shanmugam, 2000, for a critical review), reliable genetic interpretations for buried deep-marine deposits have been done based on high-quality seismic data (e.g., Gee *et al.*, 2007; Back *et al.*, 2011; Jiang *et al.*, 2012; Sylvester *et al.*, 2012).

The present paper applied the methodology of seismic facies analysis and seismic geomorphology to the Eocene interval of northern Santos Basin, in order to characterize the depositional architecture of a strongly progradational shelf-margin. Emphasis is on depositional and erosive features developed in the outer shelf, slope and basin with the objective of determining the spatial and genetic relationships among different sediment dispersal systems.

REGIONAL SETTING

The Santos Basin is located in the southeastern Brazilian margin and is limited in the north by the Cabo Frio High and in the south by the Florianópolis High (Fig. 1). Basin evolution is related to the break-up of Gondwana and opening of the South Atlantic Ocean, including an early Cretaceous rift and a late Cretaceous to modern divergent margin (Moreira *et al.*, 2007). Remarkable was the development of a late Aptian evaporitic phase, during which very thick halite deposits accumulated in a restricted marine environment (Dias, 2008). Subsequent displacement of salt played an important role creating depocenters and structural highs for post-salt deposition.

After a maximum marine flood in the Turonian, isostatic adjustments on the continental margin resulted in the Serra do Mar uplift. Denudation of this mountain range increased sediment supply to the basin and started an extensive regressive phase (Juréia progradation; Macedo, 1989), which persisted through the Eocene (Mohriak & Magalhães, 1993) (Fig. 1). Sediment load associated with progradation contributed to the offshore movement of salt and for the generation of important structures in the basin (Sombra *et al.*, 1990; Assine *et al.*, 2008; Badalini *et al.*, 2010).

The Eocene interval, object of the present study, comprises the uppermost section of the Juréia progradation. In addition to uplifting and denudation, this period was the stage for a dramatic climate warming (Eocene thermal maximum; Lourens *et al.*, 2005) that increased rainfall in the hinterland and contributed to intensify the sediment supply (Zalán & Oliveira, 2005). In northern Santos Basin, the high-sediment input during the Eocene was controlled by the Paraíba do Sul paleodrainage system (Modica & Brush, 2004; Ribeiro, 2007). Due to this combination of climatic and tectonic controls, high-relief slope clinoforms with thin to truncated topsets are the most common depositional geometry of the Eocene. In slope-to-basin areas, expressive muddy and sandy deposits associated with sediment gravity flows have formed and can be identified in different stratigraphic levels within the clinoform packages (d'Ávila *et al.*, 2008).

The end of the Eocene records another important climate change, when a global cooling altered the rainfall regime (Sahy *et al.*, 2015). In addition to that, tectonic adjustments in the Serra do Mar range caused a reorganization of the drainage system, leading Paraíba do Sul River to migrate north and to start delivering its load to Campos Basin (Karner & Driscoll, 1999). As a result, a dramatic reduction in sedimentation rate took place in northern Santos Basin, leading to transgression and reworking by bottom currents (Duarte & Viana, 2007).

DATASET AND METHODS

The study area is located in northern Santos Basin, approximately 150 km offshore from the city of Rio de Janeiro (Fig. 2). Database was provided by the Brazilian National Agency of Petroleum, Natural Gas and Biofuels (BDEP-ANP) and consists of 20 two-dimensional (2D) seismic lines with approximately 2,300 km^2 of total coverage, including data from surveys 0228 Santos 11A, 0231

Santos 18A, 0247 Cabo Frio 3A, 0261 VB99 2D BMS, and R0003 0259 2D SPP 2Q 1999, approximately 50 km^2 of a three-dimensional (3D) seismic volume (survey 0276 BS500), and composite logs of ten exploratory wells (Fig 2).

Seismic facies analysis consists of the visual determination of three-dimensionally-recognizable reflection patterns, represented by their amplitude-, geometry- and continuity-related characteristics, and by general trends of reflector terminations (e.g., Mitchum Jr. *et al.*, 1977a, 1977b; Veeken & Van Moerkerken, 2013). According to Posamentier *et al.* (2007), seismic geomorphology consists of the interpretation of ancient geomorphic features in the subsurface using 3D

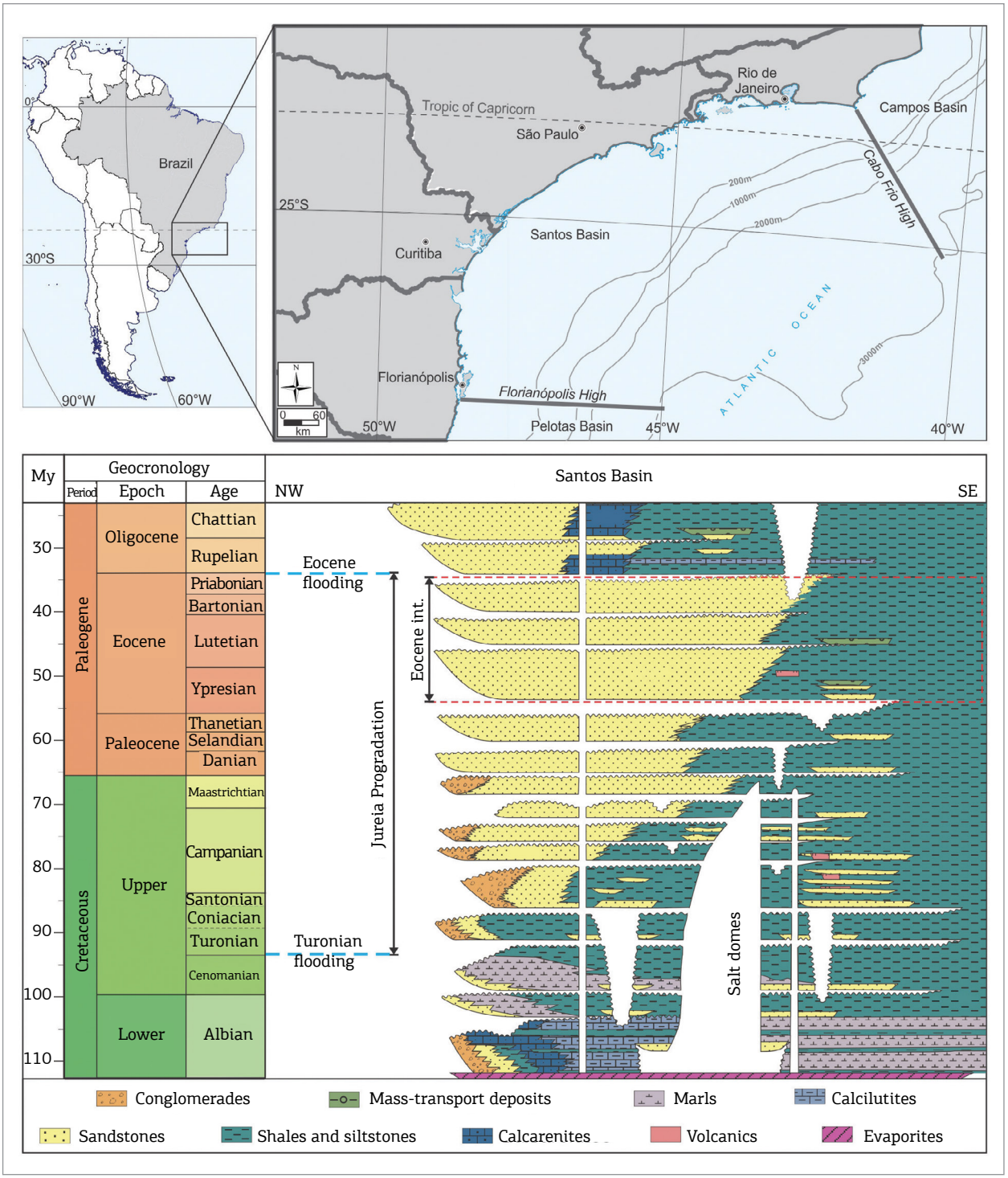

Figure 1. Location map of the Santos Basin in the southeastern Brazilian margin, and stratigraphic chart of the post-rift interval (adapted from Moreira et al., 2007).

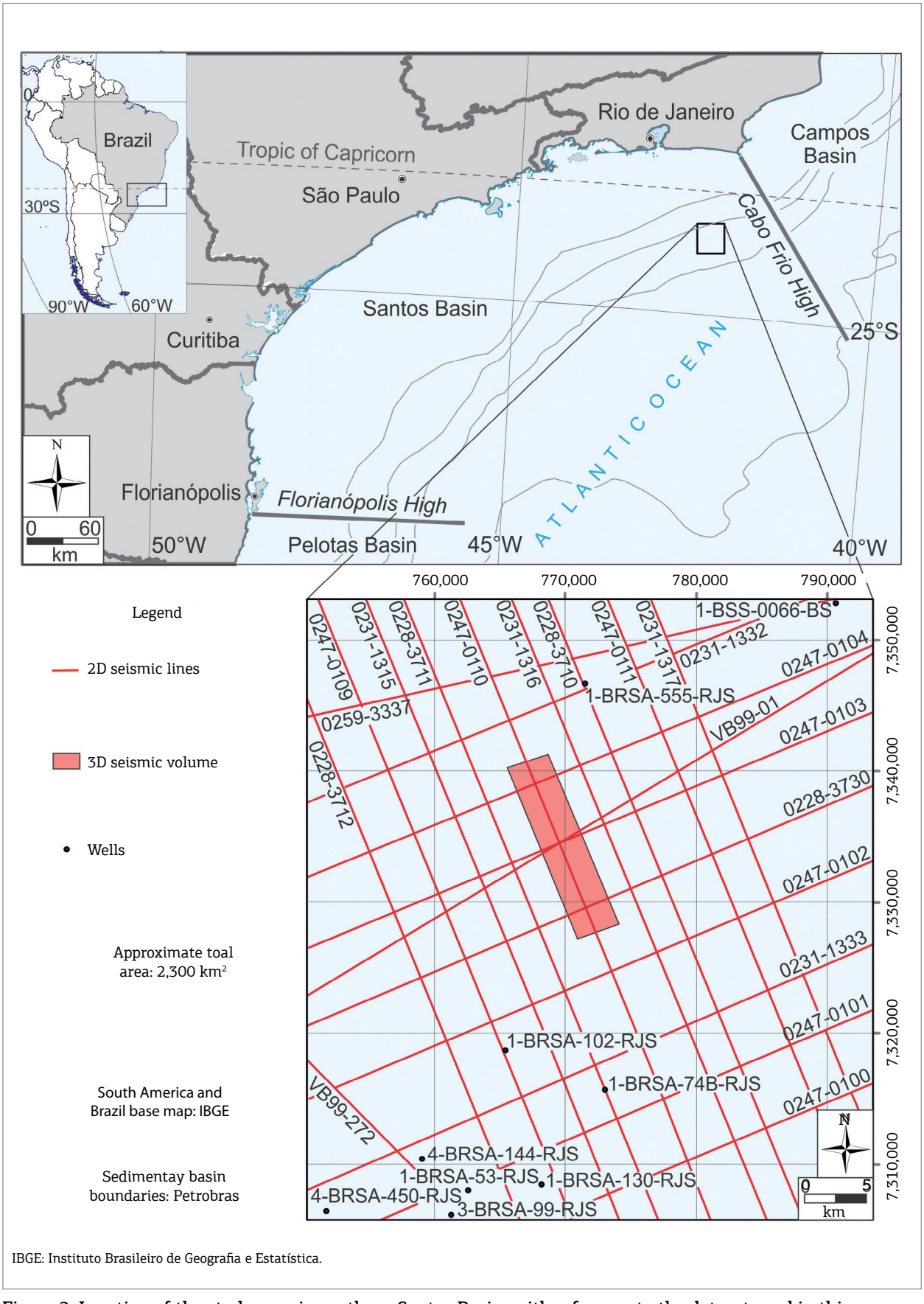

IBGE: Instituto Brasileiro de Geografia e Estatística.

Figure 2. Location of the study area in northern Santos Basin, with reference to the dataset used in this paper.

seismic data. The interpretation of these geomorphic features, along with the recognition of the environmental setting of the analyzed interval (Hadler-Jacobsen *et al.*, 2007), allows the determination of the paleogeomorphological evolution through time (Prather *et al.*, 2012).

In this study, seismic facies analysis and seismic geomorphology were complemented by the analysis of shelf-edge trajectories (e.g., Steel & Olsen, 2002; Henriksen *et al.*, 2011) in order to determine base-level fluctuations during the deposition of each of the seismic facies recognized.

SEISMIC FACIES

The Eocene interval in the study area ranges in thickness from approximately 460 m in proximal (shelf) and distal (basin) areas, to approximately 1,000 m at the slope-accretion prisms. The basal boundary of the interval is a downlap surface with predominantly low-seismic amplitudes that limits the top of the Paleocene interval (Fig. 3). The upper boundary (Eocene–Oligocene limit) is a truncation surface with predominantly high-seismic amplitudes at the study area (Fig. 3).

Six main seismic facies were recognized (Fig. 4), including prograding clinoforms, subparallel reflectors in the topset domain, high-amplitude reflectors at the bottomset of clinoforms, and mound-shaped chaotic bodies associated with high-angle truncation surfaces. Clinoform classification took into account their geometry, using an adaptation of the classification system of Mitchum Jr. *et al.* (1977a) and Berg (1982) (Fig. 5). This system considers reflection patterns for fluvial- and wave-dominated deltas, in geometries such as oblique (tangential), complex oblique, sigmoid, complex oblique sigmoid, oblique (parallel), and shingled. As most clinoforms in the studied area are limited above by truncation surfaces, clinoforms with truncated topsets but recognizable sigmoidal geometries are referred to as "sigmoid clinoforms", because of the clear geometric differences when compared to "oblique (tangential) clinoforms" (Fig. 5).

It is important to consider that clinoforms in seismic data are depositional forms with dimensions varying from few hundreds of meters to several kilometers (slope-accretion clinoforms; Steel & Olsen, 2002; Johannessen & Steel, 2005). Slope-accretion clinoforms are composed of topset, foreset and bottomset domains. The topset corresponds to the continental to shelfal domain, extending to the shelf margin and encompassing reflectors that dip in very low angles towards the basin (Safronova *et al.*, 2014). An inflexion marks the shelf break, when gradients become steeper in slope areas (foreset domain). At the slope toe, a new gradient change marks the decrease in dip angles, in the transition between slope to basin, and beginning of the bottomset domain.

Within these domains, depositional elements and erosive features were interpreted based on morphological characteristics identified in seismic sections, and on modern examples described in the literature, following the orientations by Stow and Mayall (2000) for sub-surface studies. The term

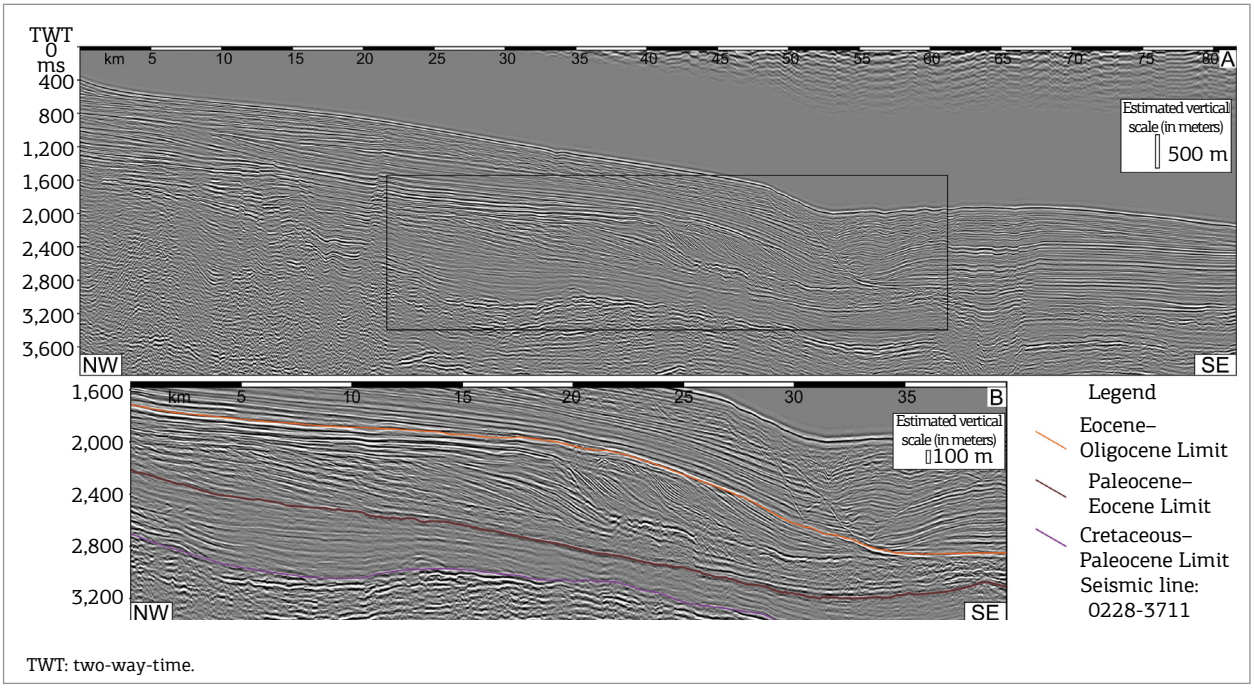

Figure 3. Interpreted 2D, dip-oriented seismic section highlighting the major seismic horizons of the studied interval.

clinoform set is an informal classification used here to define groups of clinoforms with similar geometric characteristics, limited above and below by localized truncation surfaces and their downdip equivalent surfaces (e.g., Sydow *et al.*, 1992). The term *mass-transport deposit* (MTD) is used in this text as a reference to mud-rich chaotic deep-marine deposits related to slumps and debris flows (e.g., Weimer, 1989; Omosanya & Alves, 2013; Alves *et al.*, 2014; Deckers, 2015).

Seismic facies A

This facies is composed of small-sized oblique (tangential) and complex sigmoid-oblique clinoforms, with maximum

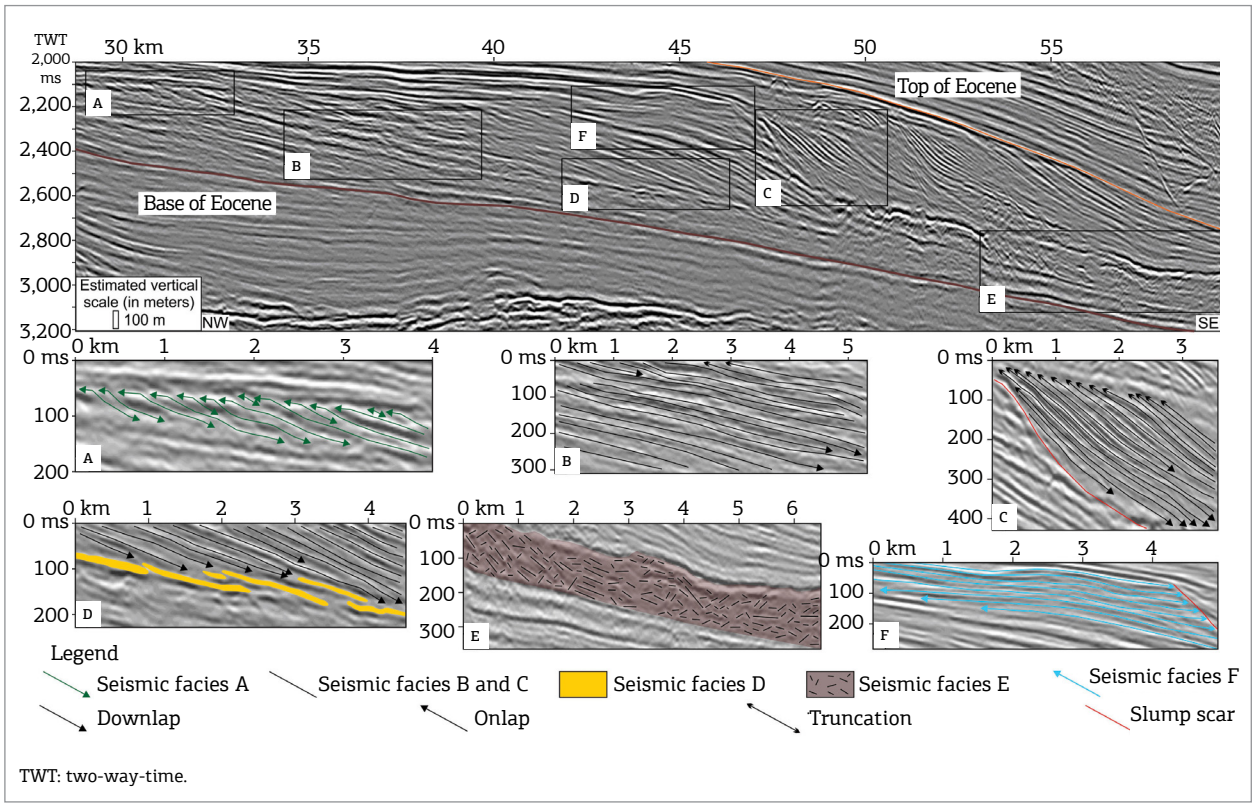

Figure 4. Main seismic facies recognized in the Eocene interval in northern Santos Basin. (A) Seismic facies A, interpreted as shelf-margin deltas/shoreface deposits; (B) seismic facies B, interpreted as slope clinoforms with tangential (oblique) geometry; (C) seismic facies C, interpreted as slope clinoforms with sigmoidal geometry; (D) seismic facies D, interpreted as turbidites; (E) seismic facies E, interpreted as mass-transport deposits; (F) seismic facies F, interpreted as continental to shelfal deposits.

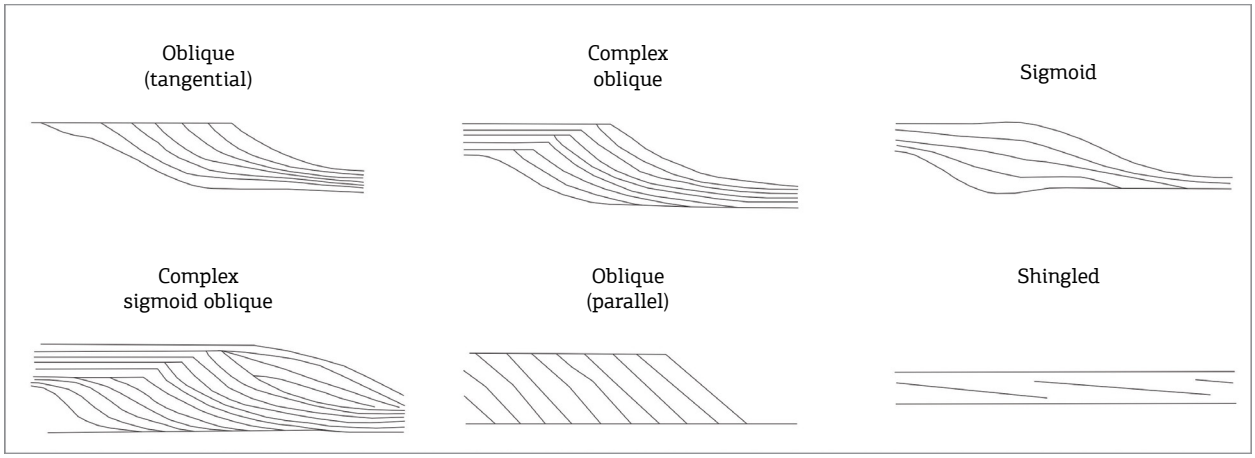

Figure 5. Classification of clinoforms based on geometric configuration, as suggested by Mitchum Jr. et al. (1977a) and Berg (1982).

relief reaching 200 ms two-way-time (TWT) (approximately 250 m) and maximum longitudinal extension of 3 km (Fig. 6). Seismic amplitudes are moderate to high, and in many cases a transition of high acoustic impedance contrasts on topsets to low contrasts on foresets, and bottomsets is observed (Fig. 6). Topsets are generally truncated (toplap terminations), with flat to descending trajectories of the clinoform rollover (Fig. 6). Foreset angles vary from 4º to 5º.

This facies is interpreted as shelf-margin deltas (e.g., Porębski & Steel, 2003; Moreira & Carminatti, 2004; Patruno *et al.*, 2015) or shoreface deposits (e.g., Bourget *et al.*, 2014) formed when sand-rich progradational systems advanced beyond the original shelf edge. In seismic data, both deposits appear as smaller-scale prograding clinoforms, and in well data both show a sand-rich composition. Shelf-edge trajectories, long-term progradation and thin to truncated topsets indicate that the progradation was influenced by high-sediment supply in periods of stationary to falling base level. Acoustic impedance contrast variations indicate a transition from sandy proximal deposits to muddy distal deposits which, in many cases drape onto high-relief oblique clinoforms.

Seismic facies B

This facies is composed of high-relief oblique (tangential) clinoforms with relatively low angles (up to 2º), longitudinal extension reaching 15 km, and maximum relief of 800 ms TWT (approximately 1,000 m; Fig. 7A and 7B). A gentle increase in slope dip angles is observed from the oldest to the youngest clinoforms, from approximately 1º up to 2º (Fig. 7A and 7B). Topsets are generally truncated, and trajectory of clinoforms rollover is slightly (when topsets are preserved) to strongly descending (when topsets are truncated; Fig. 7B). Seismic amplitudes are generally high in topset areas, but a transition to low amplitudes in bottomset areas can also be identified. In some cases, seismic amplitude peaks are verified in the foresets. Frequency of the reflections varies from low to moderate.

In many cases, these high-relief clinoforms are contiguous to the shelf-margin deltas/shoreface deposits (seismic facies A), being interpreted as low-angle tangential (oblique) slope clinoforms (e.g., Porębski & Steel, 2003; Johannessen & Steel, 2005; Patruno *et al.*, 2015). Descending trajectories and truncated topsets indicate that their genesis is related to periods of relative sea-level fall. Variations of seismic amplitudes are associated to the transition from proximal sandy deposits to distal muddy deposits, while amplitude peaks in foreset areas suggest the occurrence of intra-slope (shingled) sand-rich turbidites (e.g., Johannessen & Steel, 2005).

Despite the lack of well control and/or 3D seismic data to reinforce the interpretation of such accumulations, sand concentration on slope areas is generally associated to channel and/or canyon filling (e.g., Carvajal & Steel, 2006). The gradual increase in foreset dip with time may be related to a progressive increase on sediment supply, as a consequence of relative sea level fall and erosion in the shelfal domain (Zecchin & Catuneanu, 2013).

Seismic facies C

This is the most characteristic seismic facies in the study area, and is composed of high-relief (up to 700 ms TWT; approximately 875 m) sigmoidal clinoforms, with maximum longitudinal extension of 15 km (Fig. 7C and 7D). Dip angles slightly decreases from the older to the youngest clinoforms (from 9º to 6º). Seismic amplitudes are high on foreset areas and low to moderate on the bottomsets, and frequency of the reflections is moderate to high. In most cases, topsets are truncated, and shelf-edge trajectories are descending (Fig. 7D).

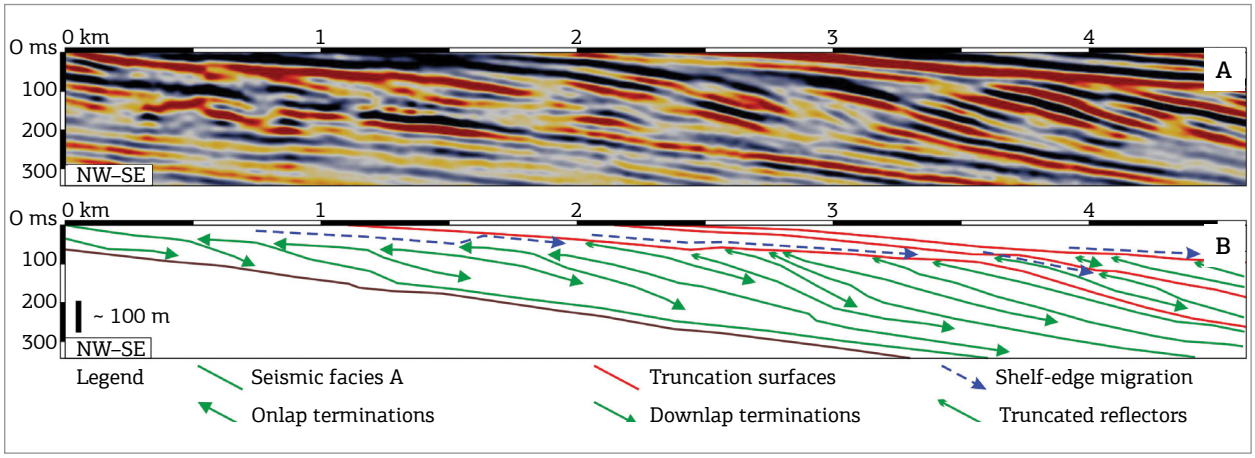

Figure 6. Seismic expression and linedrawing of seismic facies A (interpreted as shelf-margin deltas/shoreface deposits), as seen in a dip-oriented section from the 3D volume.

Clinoforms from seismic facies C are interpreted as sigmoidal slope clinoforms (e.g., Porębski & Steel, 2003; Johannessen & Steel, 2005; Patruno *et al.*, 2015), deposited during base-level falls. The external geometry of the clinoform sets is of high-relief slope-accretion prisms, limited on the top by subaerial unconformities (Fig. 7D). The accretion prisms were formed from steep physiographies, in most cases associated to high-angle truncation surfaces interpreted as large-scale slump scars (Fig. 7D). Variations on clinoform dip angles are interpreted as a consequence of the progressive approach to equilibrium profile from an initial steep gradient promoted by slope failure.

Seismic facies D

This seismic facies is composed of reflectors with high-acoustic impedance contrasts and low frequency, with maximum thickness reaching 40 ms TWT (approximately 50 m). Longitudinal extension is variable, ranging from 1,5 to 15 km. This facies is common on the bottomsets of slope clinoforms, being interpreted as turbidites with variable dimensions, and with a sand-rich composition (Fig. 8)

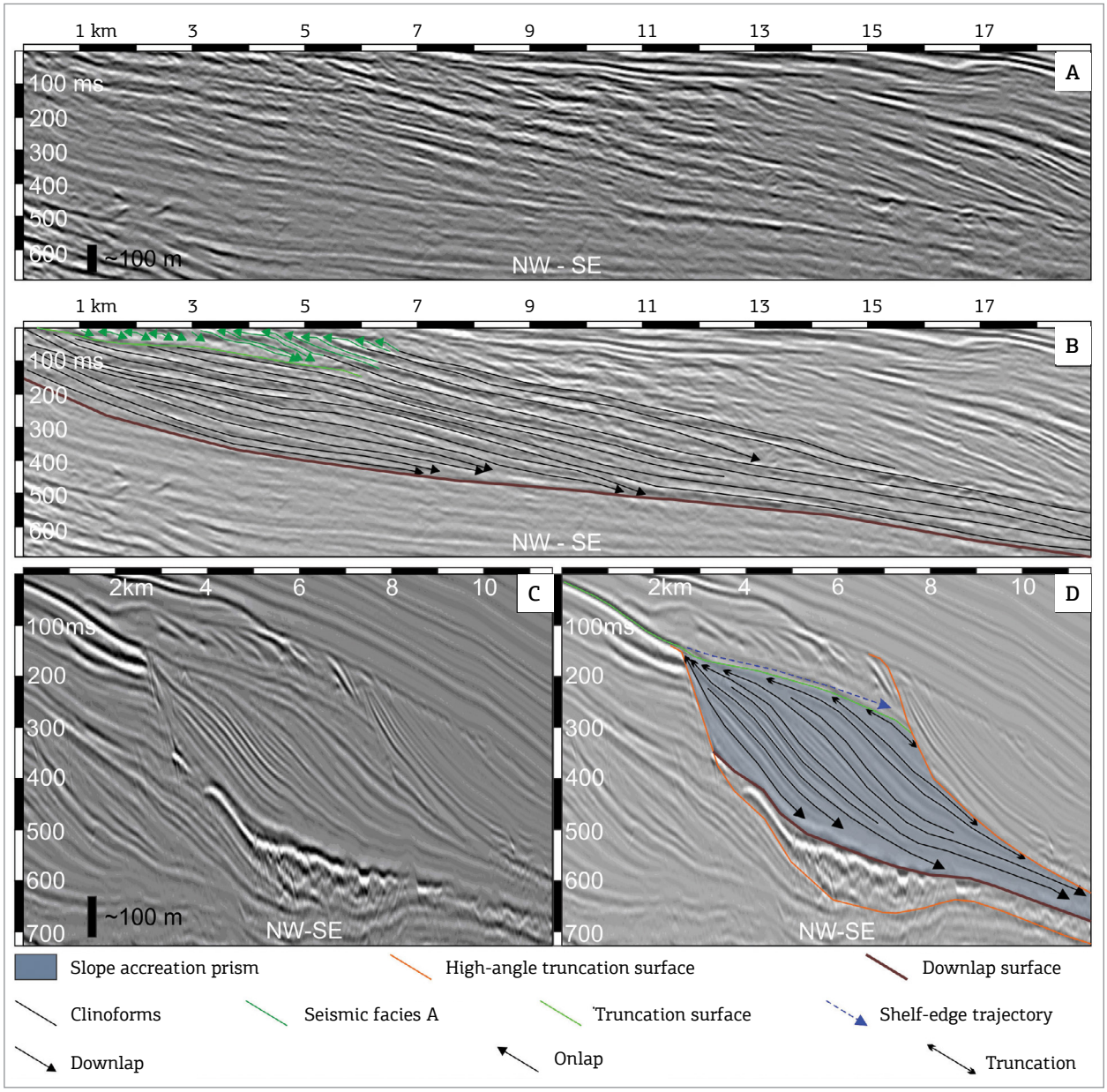

Figure 7. Different architectural patterns of slope clinoforms with flat to descending trajectories. (A, B) Oblique (tangential) clinoforms from seismic facies B, attached to shelf-margin deltas/shoreface deposits from seismic facies A; (C, D) sigmoidal clinoforms from seismic facies C, with high-angle.

(e.g., Posamentier & Erskine, 1991; Moreira & Carminatti, 2004; Johannessen & Steel, 2005).

In 3D seismic data, it is possible to observe that this facies configures channels and frontal splays (Fig. 9). Submarine channels width varies from 100 to 150 m, generally with low to moderate sinuosity and, more locally, with high sinuosity (Fig. 9A and 9B). Moreira & Carminatti (2004), using a larger 3D seismic volume than the one used in the present paper, recognized a meandering pattern for submarine channels that compose the turbidite systems. Therefore, the mainly straight geometry observed in the study area may be a local characteristic.

In the terminal portions of the submarine channels, asymmetric-fan-shaped frontal splays were identified (Fig. 9). Lateral extension of the frontal splays varies from few hundreds of meters to thousands of meters. Negative acoustic impedance peaks and well information indicate a sandy composition for these deposits (Figs. 8 and 9). Sediment-feeding of these splays seem to be related to submarine canyon incision on slope areas. Canyons reach up to 35 ms TWT deep (approximately 45 m), and have a mainly straight morphology. These erosive forms acted as preferential points to clastic sediment influx to the basin (Stow & Mayall, 2000). Canyon-fill deposits display a divergent seismic configuration according to the classification by Mitchum *et al.* (1977a).

Seismic facies E

Seismic facies E has a predominantly chaotic reflector pattern, with low to moderate seismic amplitudes and high frequencies. The external form of the deposits, in strike and dip sections, is of mound-shaped bodies at the slope toe, with few to tens of kilometers of longitudinal extension (maximum of 30 km; Fig. 10). The chaotic pattern is interpreted as mass-transport deposits (e.g., Posamentier & Kolla, 2003; Martinez *et al.*, 2005; Alfaro & Holz, 2014).

In well data, the chaotic facies is described as of gravelly mudstones (diamictites) or mudstones with sand interbeds. Internally, this facies is strongly affected by sin-sedimentary deformation, more typically reverse faults pointing to a compressive regime (Fig. 10; e.g., Posamentier & Kolla, 2003; Posamentier & Martinsen, 2011). Other compressive structures, such as open folds (Fig. 10), are observed both in 2D seismic lines and in the 3D seismic volume, being comparable to examples reported in the literature (e.g., Martinez *et al.*, 2005; Moscardelli *et al.*, 2006; Alfaro & Holz, 2014).

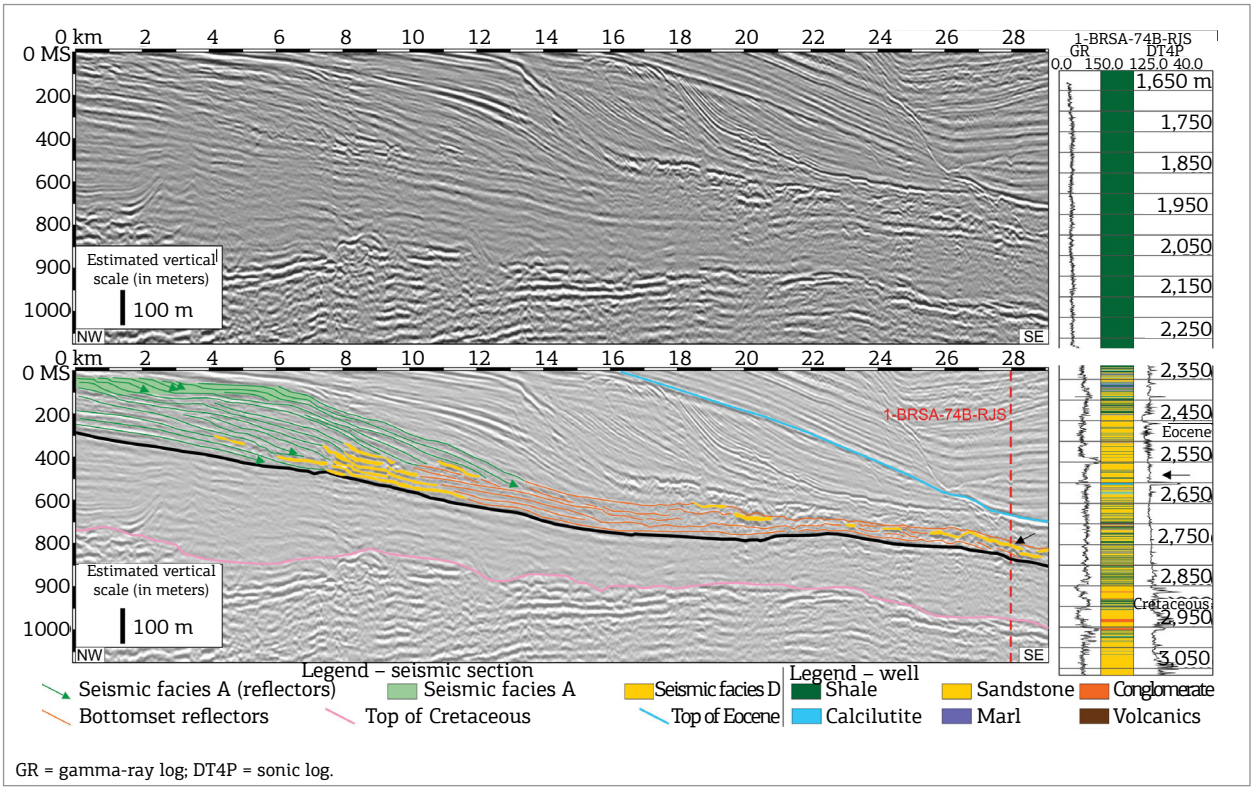

Figure 8. 2D seismic section and line drawing highlighting sandy turbidites in the bottomsets of slope clinoforms. Note the association between seismic facies D (interpreted as turbidites) and seismic facies A (interpreted as shelf-margin deltas/shoreface deposits, shown as green reflectors in the topset domain). The well log to the right shows sand-rich deposits (indicated by a black arrow) associated to the seismic facies interpreted as turbidites. Figure adapted from Berton and Vesely (2016).

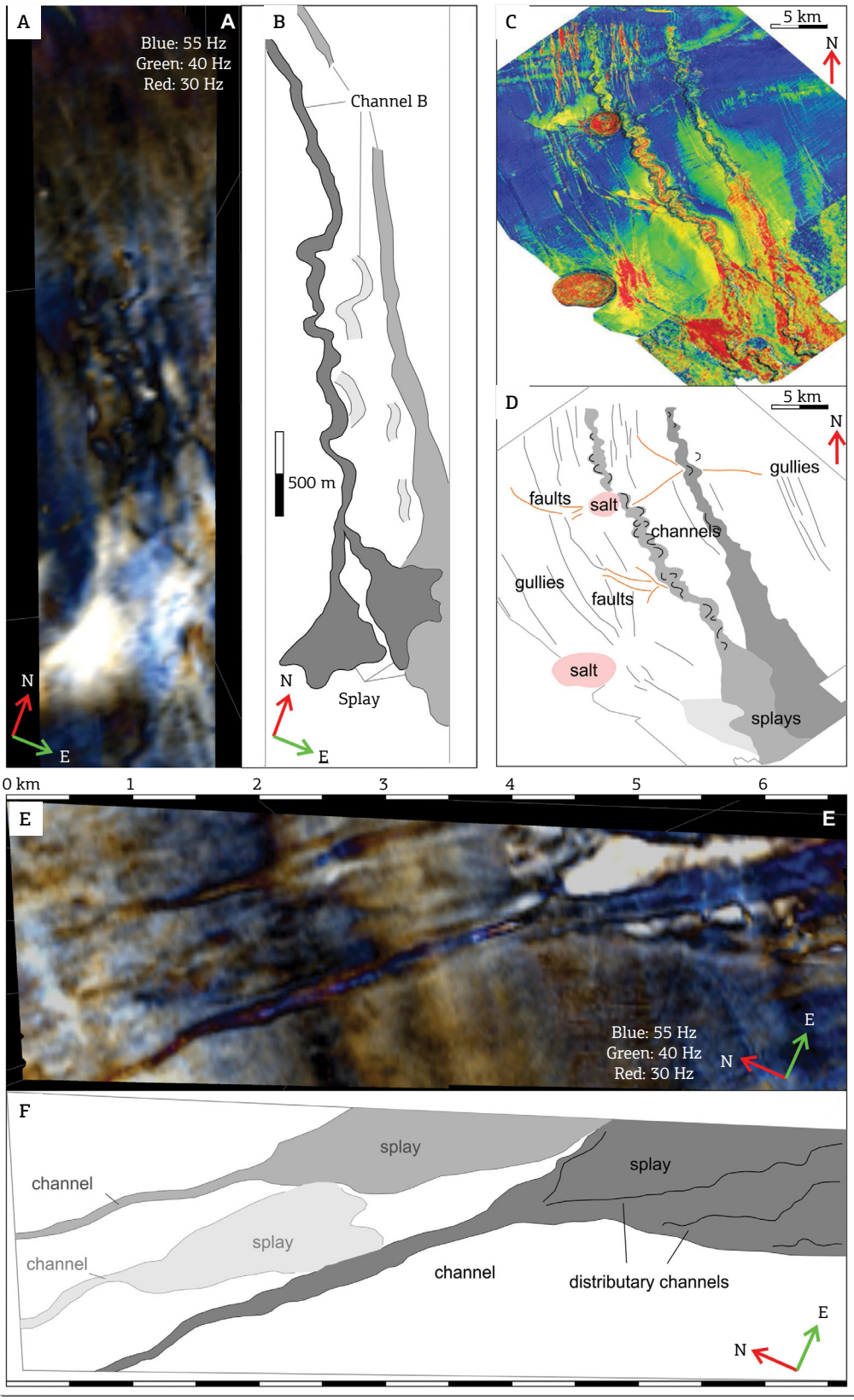

Figure 9. Spectral decomposition maps showing sets of submarine channels and frontal splays that compose the high-amplitude seismic facies D (interpreted as turbidites) at the bottomset of oblique tangential clinoforms from seismic facies B (A, E). These systems are interpreted in (B) and (F). See Fig. 2 for the location of the 3D volume in the study area. (C, D) Submarine channels and fans as identified by Sylvester *et al.* (2012) in the Pleistocene of the Gulf of Mexico. Note the similarity with the channels and frontal splays identified in the present paper.

Isopach maps for the two largest MTDs show a maximum thickness of 135 ms TWT (approximately 170 m) and a longitudinal extension of 30 km for MTD 1 (Fig. 11). Thickness variation in MTD 1 is subtle, but larger thicknesses are concentrated in its northwestern portion. This pattern is also observed in the smaller deposit (MTD 2), but in this case the chaotic facies is restricted to the central to northwestern part of the deposit and not observed in the SE domain. The third MTD, associated to a smaller slump scar, was not mapped, as it is observed only in few strike sections.

The MTDs are associated to three major slump scars and the generation of these deposits is interpreted as related to the gravitational collapse of the slope (Figs. 10 and 12). Relief of the slump scars vary from 420 to 550 ms (525–690 m, approximately), while their longitudinal extension vary from 3.0 to 3.7 km, resulting in a steep topography with angles exceeding 10º. In the upper slope, the scars are truncated by unconformities, and basinward they are contiguous to the basal detachment surfaces of the MTDs (Fig. 12). Reflectors with more lateral and longitudinal continuity and higher amplitudes are also associated with the chaotic facies (Fig. 10). These are interpreted as low-deformed sand-rich slipped blocks, transported as rafts within the mass flow (Fig. 10; e.g., Gamboa *et al.*, 2012; Alfaro & Holz, 2014). The rafted blocks are concentrated in the upper part of the MTDs, but they also occur in the middle part or directly on the basal detachment surfaces.

Seismic facies F

This facies is composed of topset reflectors with subparallel to divergent pattern, with moderate to high amplitudes

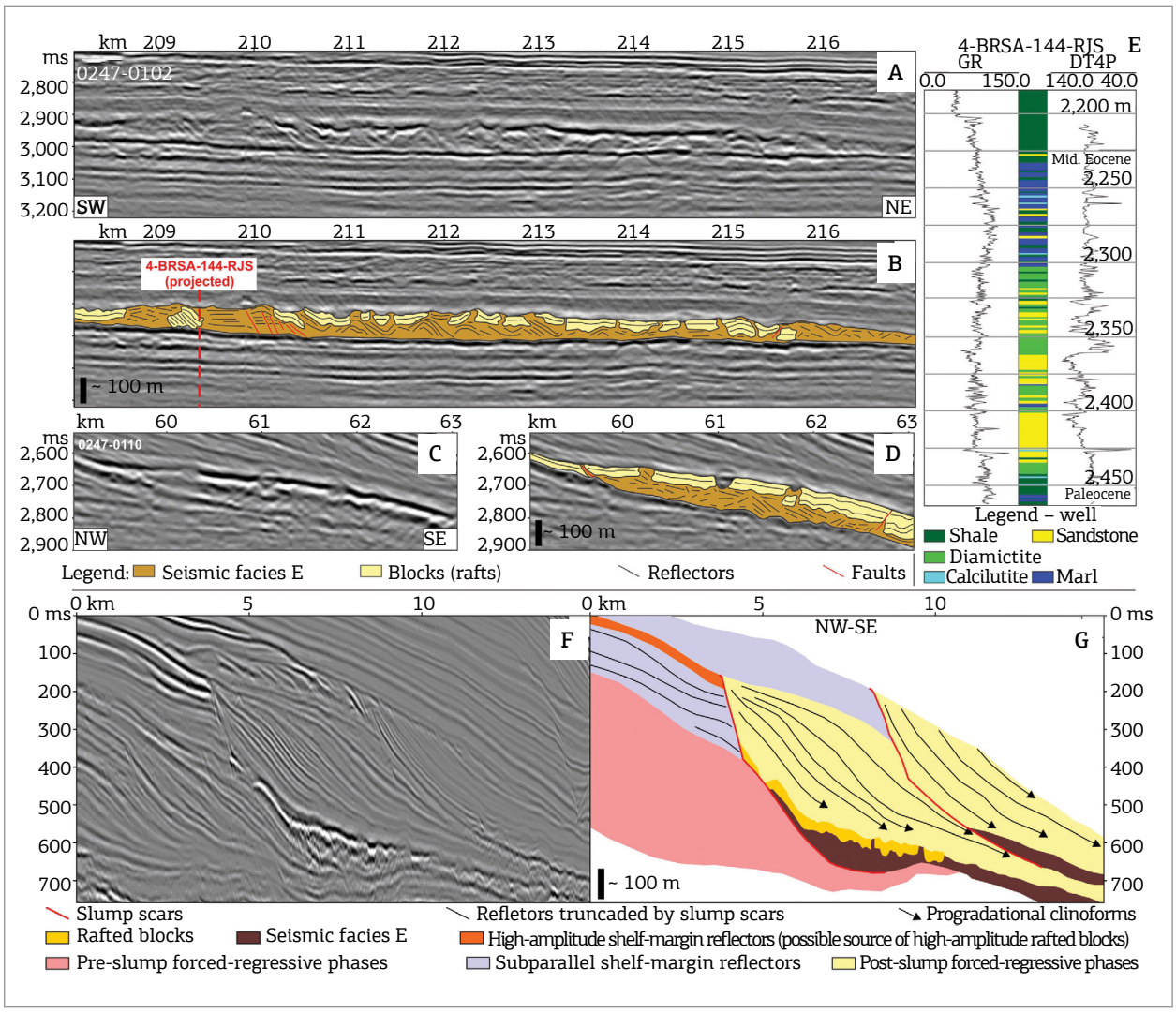

Figure 10. Seismic facies E, interpreted as mass-transport deposits, as seen in strike (A and B) and dip (C and D) sections. Note that regardless the main chaotic configuration, folded, faulted, arched and subparallel reflectors are also observed. High-amplitude rafted blocks collapsed from the shelf margin are concentrated near the top of the deposits. E and F illustrates that MTDs are overlain by sigmoidal clinoforms (seismic facies C) that postdate the slump scars. Figure adapted from Berton and Vesely (2016).

and high frequency (Fig. 13). Onlap terminations of the reflectors migrate toward the continent, while basinward they are truncated by the slump scars (Fig. 13). The maximum thickness of these topset deposits is about 300 ms TWT (approximately 375 m), recording extensive periods of aggradation on the shelf. They are probably constituted of non-marine (coastal plain) to outer shelf deposits, formed in periods of positive accommodation in the shelf related to rising base-level and high sedimentation rates (normal regressions).

Seismic facies associations

Seismic facies were grouped in genetic associations (Fig. 14) that reflect the environmental conditions during deposition. Association 1 is composed of shelf-margin deltas/shoreface deposits (seismic facies A), tangential (oblique) slope clinoforms (seismic facies B) and sand-rich turbidites (seismic facies D). In association 2, only sigmoidal slope clinoforms from seismic facies C and turbidites from seismic facies D have been identified. Association 3 is composed only by seismic facies F, with subparallel to divergent topset reflectors. Association 4 is composed of chaotic bodies from seismic facies E, sigmoidal clinoforms from seismic facies C and turbidites from seismic facies D.

The characteristics of the seismic facies that compose the interpreted facies associations allow the assessment of the depositional conditions acting during the deposition of each association. Association 1 represents periods of relatively high sediment supply and stationary to falling base level, with the development of long-term progradations and deposition of thick and extensive turbidites. In the younger part of the association shelf-margin deltas/shoreface deposits are rarer than in the older part, and low-angle tangential (oblique) slope clinoforms with truncated

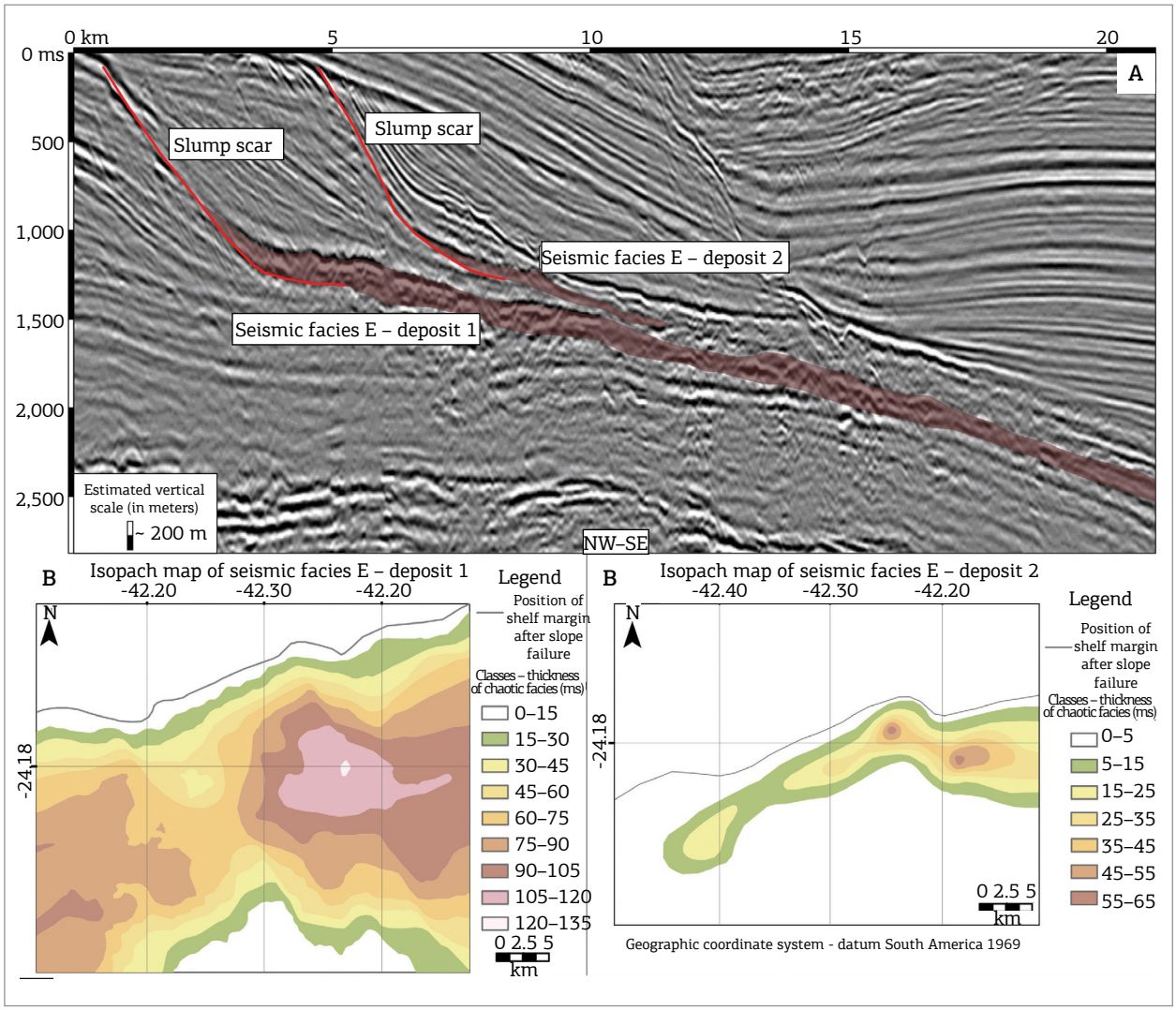

Figure 11. Dip-oriented section and isopach maps representative of the two main MTDs identified in the study area. Figure adapted from Berton and Vesely (2016).

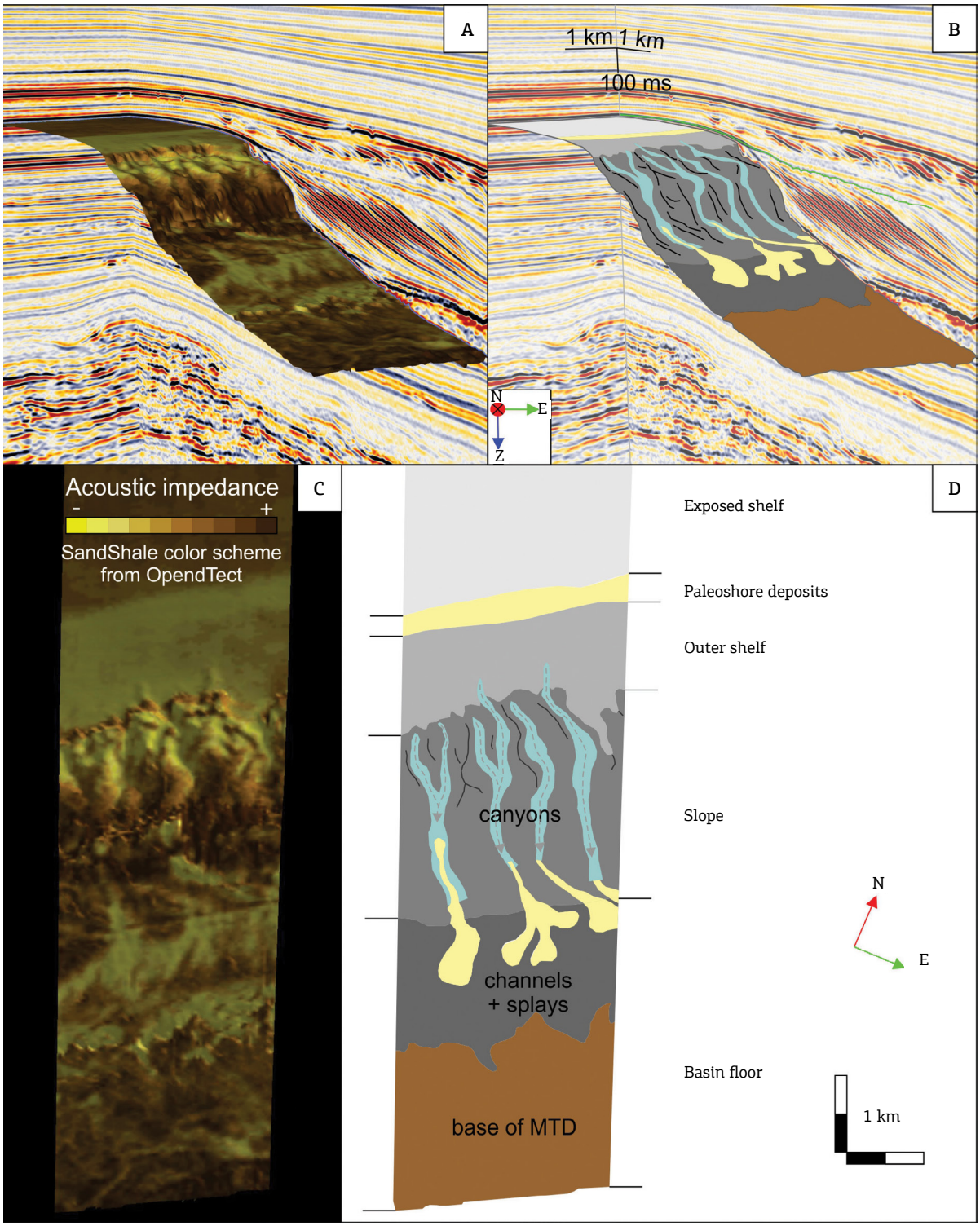

MTD: mass-transport deposit.

Figure 12. Amplitude map of the seismic horizon that comprise the lower boundary of MTD 1 (lower foreset to bottomset) and its correspondent slump scar (upper foreset) in perspective (A, B) and plan view (C, D). Note that the slump scar is cut by canyons that feed sand-rich splays at the lower slope.

topsets and turbidites are predominant. This configuration is coherent to a period of falling sea-level, when shelf-margin deltas/shoreface deposits were eroded. Despite the relative low angle of the slope clinoforms, a gradually steeper slope is built from the older part of the association to the younger one. Gradients considerably increase in association 2, in which the predominant geometry is of high-angle sigmoidal slope clinoforms with truncated topsets, and with sand-rich turbidites in the bottomsets, deposited during base-level falls.

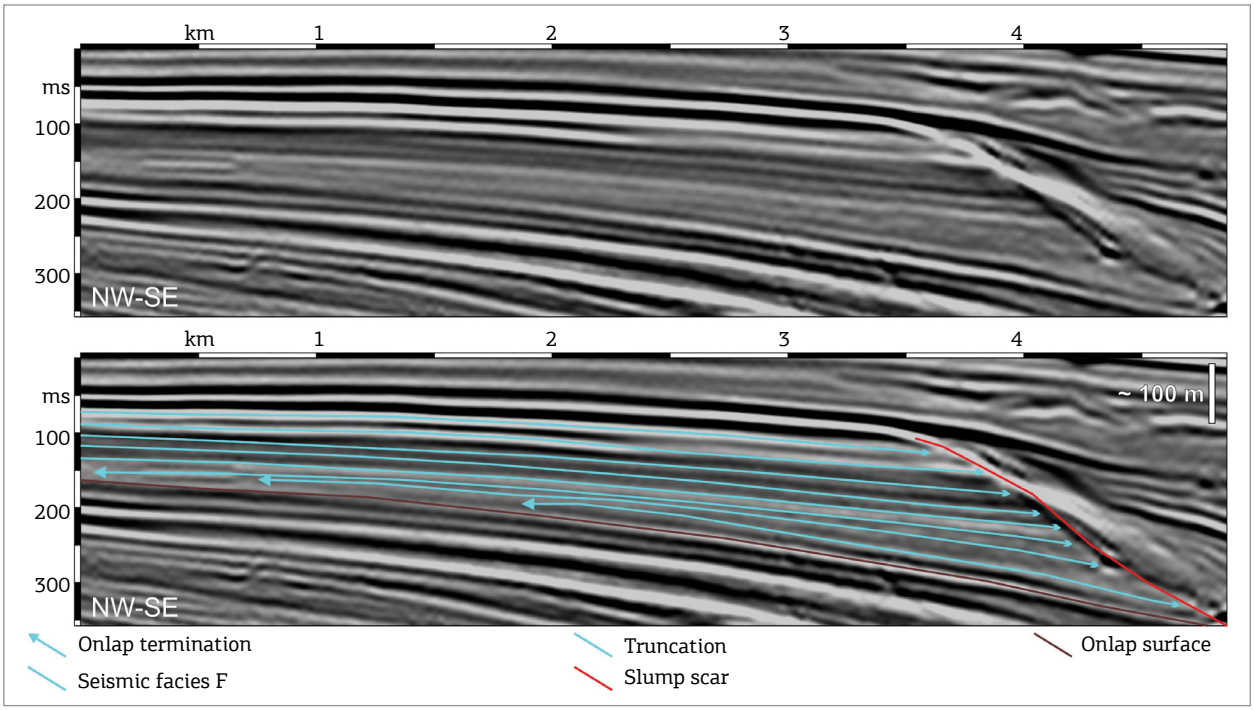

Figure 13. Dip-oriented seismic section showing subparallel to divergent reflectors from seismic facies F, on the topset domain and with onlap terminations migrating towards the continent. Basinward, these are truncated by a slump scar.

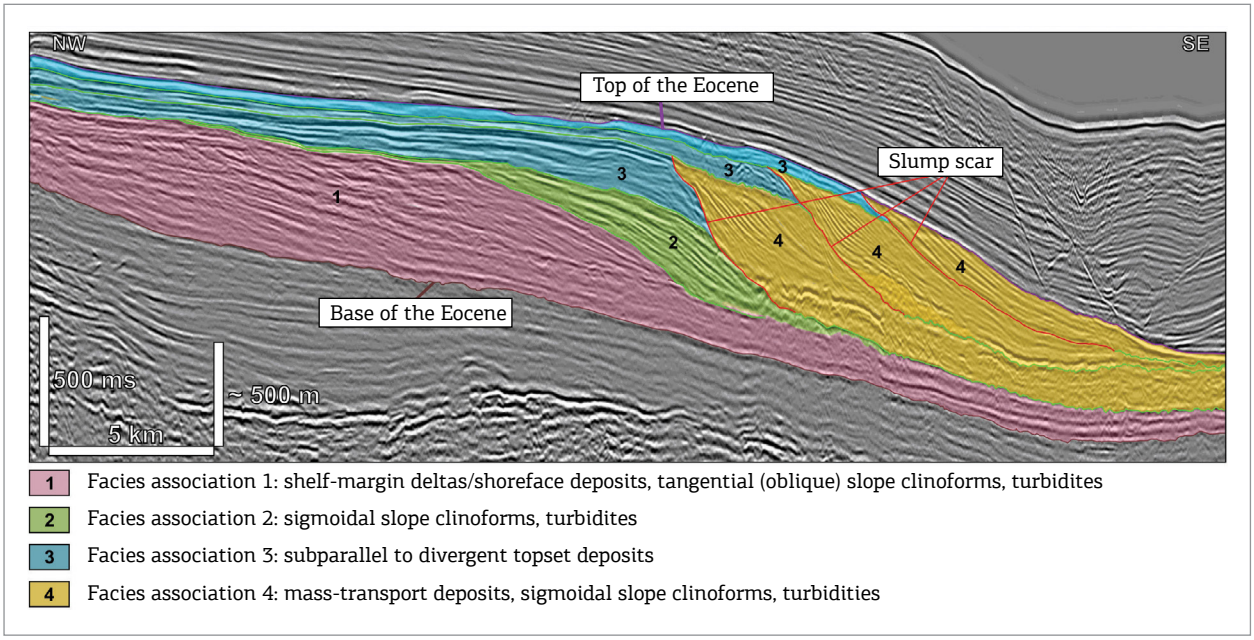

Figure 14. Dip-oriented seismic section highlighting genetically associated seismic facies. Each facies association represents a depositional interval when conditions of sediment supply and relative sea-level were relatively constant.

Association 3 records a period of relative sea-level rise, when aggrading deposits associated to normal regressions were deposited in the shelf. The aggradational phases culminate in the slope gravitational collapse and consequent generation of chaotic deposits interpreted as MTDs. As a consequence, these deposits configure the basal part of association 4, overlapped by high-angle sigmoidal slope clinoforms and sand-rich turbidites. The seismic facies from association 4 are coherent to periods of base-level fall, following periods of base-level rise and deposition of aggradational reflectors from association 3. Consequently, slope collapse marks the onset of base-level fall.

DISCUSSION

The studied interval is dominated by prograding clinoforms with few aggradation (Figs. 4, 7 and 14), indicating conditions of forced regressions and relatively high sediment supply (e.g., Zecchin & Catuneanu, 2013). In this context, seismic facies associations with their related depositional elements and erosive features represent tridimensional depositional intervals characterized by specific paleoenvironmental conditions and associated base-level behavior (Fig. 14).

High-sediment supply and forced regressions are favorable for the development of shelf-margin deltas (Mellere *et al.*, 2002), but in such conditions, prograding shoreface deposits may result in a similar seismic facies. In the studied interval, seismically detectable shelf-margin deltas/shoreface deposits are concentrated in the first seismic facies association, being sparse in the remaining ones (Figs. 4, 6 and 14). This characteristic is possibly a consequence of erosion of these deposits during extensive periods of exposure of the shelf margin, associated to base-level falls (Mellere *et al.*, 2002). In these periods, the knick-points of canyons developed on slope areas may migrate landward and become connected to shelf-incised fluvial systems, preventing the generation of shelf-margin deltas (Kolla & Perlmutter, 1993). Such connection was suggested by Moreira & Carminatti (2004) in their analysis of canyons developed during the Eocene in northern Santos Basin.

Oblique (tangential) slope clinoforms (seismic facies B) and sand-rich turbidites (seismic facies D) occur in association with the shelf-margin deltas/shoreface deposits (seismic facies A). The increase on dip angles from older to youngest slope clinoforms (Fig. 7B) in association 1 suggests an increase in sediment supply and sediment caliper as a result of base level fall and erosion on the shelf (e.g., Zecchin & Catuneanu, 2013; Safronova *et al.*, 2014). While in the first parts of association 1, lower-angle slope clinoforms (maximum slope angle of approximately 1º) are associated to flat to mildly descending shelf-edge trajectories, steeper clinoforms in the last stages of the association (maximum slope angle reaching 2º) are related to strongly descending trajectories (Figs. 7 and 14). Consequently, shelf-margin deltas/shoreface deposits are abundant in the older stages of association 1, and rarer in the younger ones which were formed during a more expressive phase of base level fall (Fig. 14). Slope angle increase in this depositional interval is a consequence of extensive forced regressions that caused the migration of the sediment input points to areas closer to the shelf margin and upper slope (Catuneanu, 2006; Catuneanu *et al.*, 2009).

Although sand transport to the deep-sea is favored by forced regressions (e.g., Muto & Steel, 2002; Helland-Hansen & Hampson, 2009), occurrence and volume of turbidites are not exclusively controlled by base-level falls (e.g., Burgess & Hovius, 1998; Plink-Björklund & Steel, 2002; Carvajal & Steel, 2006; Dixon *et al.*, 2012; Safronova *et al.*, 2014; Berton & Vesely, 2016). Turbidites were identified in all seismic facies associations formed during base-level falls, but they are more frequently observed on the bottomset of clinoforms from association 1, in which well-developed shelf-margin deltas/shoreface deposits occur (Figs. 4 and 8). Based on similar observations, Moreira & Carminatti (2004) divided the Eocene deep-water deposits in north Santos Basin in a sand-rich domain — corresponding to association 1 in the present paper —, and a mud-rich domain, equivalent to association 4 (Fig. 14). Sand-rich turbidites are also identified in facies associations corresponding to the mud-rich domain of Moreira & Carminatti (2004), but MTDs associated with submarine slumps in these associations probably prevented the formation of well-developed submarine fans, by creating an irregular topography over the sea-floor with barriers to the propagation of the turbiditic flow (e.g., Machado *et al.*, 2004). Only in more distal parts of the basin, well-developed turbidites with high-amplitude reflectors and extensions up to 10 km are observed, subsequent to MTD emplacement.

Recurrence of submarine slumps truncating reflectors from associations 2 to 4 and the low thickness of bottomset deposits make hard to correlate these distal submarine fans to a specific depositional interval or base-level trend. However, considering the relatively high-sediment supply in relation to the mainly falling base-level trend, it seems coherent to ponder that the more distal submarine fans were fed by turbidity current during both rising and falling of relative sea level (e.g., Mutti & Normark, 1991; Burgess & Hovius, 1998; Shanmugam, 2002; Dixon *et al.*, 2012; Safronova *et al.*, 2014; de Gasperi & Catuneanu, 2014) (Fig. 14).

Therefore, the primary control on turbidite deposition was the sediment supply (e.g., Burgess & Hovius, 1998; Dixon *et al.*, 2012; Safronova *et al.*, 2014), although the influence of falling to low relative sea level was crucial to the development of shelf-margin deltas/shoreface deposits that were the

main feeders for deep-water sands (e.g., Mellere *et al.*, 2002; Johannessen & Steel, 2005; Dixon *et al.*, 2013). The architectural pattern of the turbidite systems (channels ending in frontal splays) is well known and well documented in the classic literature on deep-water systems (e.g., Mutti & Normark, 1991; Posamentier & Erskine, 1991; Shanmugam, 2000; Sylvester *et al.*, 2012; de Gasperi & Catuneanu, 2014). The mainly straight geometry of the submarine channels identified in the study area (Fig. 9) differs from the meandering pattern identified by Moreira & Carminatti (2004). However, in the Pleistocene of the Gulf of Mexico, Sylvester *et al.* (2012) identified sinuous channels confined (entrenched) within straight features (Fig. 9C and 9D). This was a result of confinement between levees that prevented a larger-scale lateral migration of the channel system. Thus, the straight character of channels observed in the present study may imply that intra-channel features are smaller than the seismic resolution.

Slope-accretion clinoforms show important geometric changes, which are a consequence of variations on depositional conditions (e.g., Saller & Dharmasamadhi, 2012; Patruno *et al.*, 2015; Fig. 7). As discussed before, an increase in the dip angles of oblique (tangential) clinoforms is observed within association 1 (Figs. 7 and 14). This increase culminated in high-relief sigmoid clinoforms with truncated topsets in facies association 2 (Fig. 14). Progradation of these clinoforms resulted in the construction of a steep gradient (approximately 6º) that probably influenced the depositional morphology of the reflectors of association 3. This association records an aggradational phase on the shelf following a relative sea-level rise, but the reflectors are truncated basinward by a slump scar (Fig. 13). The slump scar created a steep submarine physiography (exceeding 10º) that influenced the geometry of the subsequent slope-accretion clinoforms (Fig. 12). Therefore, a slope-accretion prism composed of high-relief sigmoidal clinoforms (higher than in association 2) is part of association 4 (Fig. 7 B and C).

A decrease in slope angle with time, in association, 4 records a progressive approach to the equilibrium profile, compensating the initial steep slope (e.g., Friedrichs & Wright, 2004). Considering the depositional conditions during the interval, post-slump physiography and maintenance of high-sediment supply during forced regressions controlled the geometry and high angle of the clinoforms formed just after slope failure (e.g., Zecchin & Catuneanu, 2013; Safronova *et al.*, 2014). These conditions are repeated during the interval, with new aggradation phases and formation of parallel to divergent reflectors from association 3 preceding slumps and deposition of association 4 (Fig. 14). Sigmoidal slope clinoforms from association 4 show a gradual decrease of foreset angles, in some cases from approximately 9º to 6º. The steep submarine bathymetry resultant from slope failure controlled the geometry and angles of these clinoforms, and favored the incision of straight canyons (e.g., Clausen *et al.*, 2012) (Fig. 12). These features represent preferential conduits for sediment transfer to deeper waters, and their development affected the deposition of turbidites.

The successive occurrence of submarine slumps during the interval also caused the deposition of large MTDs at the slope toe. All slumps occurred immediately after an aggradational phase composed of topset reflectors, which are the most probable source of sediments for the MTDs. Despite the relative scarcity of normal-regressive, and aggradational strata in the succession, their deposition was important for MTD generation in accumulating sediment at the shelf margin. In the case of the larger MTD, the volume of displaced shelf deposits was sufficiently large to originate a deposit with up to 30 km of lateral extent and an average thickness of about 70 ms TWT (approximately 88 m; Figs. 4 and 14). The smaller-sized MTDs are also proportional to the thickness of the precursor topset deposits (association 3), which are significantly thinner than those of the first stage of association 3 (Fig. 14). The emplacement of MTDs over sand-rich turbidites has relevance for oil exploration, as potential reservoirs (turbidites) are capped by potential seals (muddy MTDs). The sandy turbidites of the Eocene were previously recognized as good reservoirs (Moreira & Carminatti, 2004; Chang *et al.*, 2008), and oil shows associated to these deposits were detected in some wells. However, Moreira & Carminatti (2004) do not consider the MTDs as good seals due to the presence of compressive structures such as thrust faults that reduce sealing capacity (e.g., Bull *et al.*, 2009; Posamentier & Martinsen, 2011; Alves *et al.*, 2014; Fig. 10). Therefore, 3D mapping of these deformational structures, combined with petrophysical data of the diamictites, may help in the determination of the quality of these deposits as top seals.

CONCLUSIONS

Seismic facies analysis combined with seismic geomorphology and analysis of shelf-edge trajectories allowed a better understanding of the environmental conditions that operated during the evolution of the Eocene shelf-margin in northern Santos Basin:

- the geometry of strongly prograding clinoforms with thin to truncated topsets and flat to descending shelf-edge trajectories is the most common in the interval, indicating conditions of relatively high sediment supply and base level falls;
- variations of geometry and dimensions of the clinoforms were a response of equilibrium profile to conditions of sediment supply, base level fluctuations and pre-depositional submarine topography;

- moments of base-level rise and maintenance of high sediment supply caused sediment storage at the outer shelf, which was essential to subsequent slope failure;
- mud-rich MTDs with chaotic internal pattern and deformation by compressive structures are associated to slump scars;
- the geometry of high-relief clinoforms was conditioned by relatively high sediment supply and steep physiographies associated to slumps. A progressive decrease on slope gradient during progradation records approach to the submarine equilibrium profile;
- shelf-margin deltas/shoreface deposits (equivalent to seismic facies A) were efficient for the transport of sand to the deep-marine environment, as the largest volumes of sand-rich turbidites (equivalent to seismic facies D) are associated to the occurrence of seismic facies A;
- turbidite systems included channels and frontal splays. In many cases, these features are amalgamated;
- the steep physiography associated to slump scars was favorable for canyon incisions. These canyons were important for sediment-feeding of deep-marine turbiditic splays;
- turbidites have a good potential as reservoir rocks, but the compressive structures in the MTDs decrease their potential as sealing rocks.

ACKNOWLEDGEMENTS

The authors thank Universidade Federal do Paraná (UFPR) and Laboratório de Análise de Bacias (LABAP) for infrastructure and institutional support. We thank the three anonymous reviewers for constructive comments that improved the quality of the manuscript. We also thank Mario Luis Assine and Rodolfo José Angulo for their suggestions and comments in an early version of the text. Fábio Berton acknowledges the scholarship provided by the Programa Interdisciplinar em Engenharia de Petróleo e Gás Natural of UFPR (PRH-24). Fernando F. Vesely thanks the Conselho Nacional de Desenvolvimento Científico e Tecnológico (CNPq) for financial support (grants: 461628/2014-7). Seismic and well data were provided by the Agência Nacional do Petróleo, Gás Natural e Biocombustíveis (BDEP-ANP).

REFERENCES

Alfaro E. & Holz M. 2014. Seismic geomorphological analysis of deepwater gravity-driven deposits on a slope system of the southern Colombian Caribbean margin. *Marine and Petroleum Geology*, **57**:294-311. doi: 10.1016/j.marpetgeo.2014.06.002

Alves T.M., Kurtev K., Moore G.F., Strasser M. 2014. Assessing the internal character, reservoir potential, and seal competence of mass-transport deposits using seismic texture: a geophysical and petrophysical approach. *AAPG Bulletin*, **98**(4):793-824. doi: 10.1306/09121313117

Assine M.L., Corrêa F.S., Chang H.K. 2008. Migração de depocentros na bacia de Santos: importância na exploração de hidrocarbonetos. *Revista Brasileira de Geociências*, **38**(2):111-127.

Back S, Van Gent H., Reuning L., Grötsch J., Niederau J., Kukla P. 2011. 3D seismic geomorphology and sedimentology of the Chalk Group, southern Danish North Sea. *Journal of the Geological Society*, **168**:393-405. doi: 10.1144/0016-76492010-047

Badalini G., Browner F., Bourque R., Blight R., de Bruin G. 2010. Seismic-sequence stratigraphic analysis of regional 2D lines in the Santos Basin, offshore Brazil. *Search and Discovery Article*, **40538**.

Benan A.O.A.C. & Cauquil, E. 2000. Seabed morphologies and recent turbidite architectural elements as interpreted from 3D seismic data – some implications for exploration and production of the deep offshore. *In*: Appi, C.J. (Ed.). *Deep-water sedimentation:* technological challenges for the next millennium: 31st International Geological Congress. Rio de Janeiro, ABGP, p. 111-112.

Berg O.R. 1982. Seismic detection and evaluation of delta and turbidite sequences; their application to exploration for the subtle trap. *AAPG Bulletin*, **66**(9):1271-1288.

Berton F. & Vesely F.F. 2016. Stratigraphic evolution of Eocene clinoforms from northern Santos Basin, offshore Brazil: evaluating controlling factors on shelf-margin growth and deep water sedimentation. *Marine and Petroleum Geology*, **78**:356-372. doi: 10.1016/j.marpetgeo.2016.09.007

Bourget J., Ainsworth R.B., Thompson S. 2014. Seismic stratigraphy and geomorphology of tide or wave dominated shelf-edge delta (NW Australia): process-based classification from 3D seismic attributes and implications for the prediction of deep-water sands. *Marine and Petroleum Geology*, **57**:359-384. doi: 10.1016/j.marpetgeo.2014.0 5.021

Bull S., Cartwright J., Huuse M. 2009. A review of kinematic indicators from mass-transport complexes using 3D seismic data. *Marine and Petroleum Geology*, **26**(7):1132-1151.

Burgess P.M. & Hovius N. 1998. Rates of delta progradation during highstands: consequences for timing of deposition in deep-marine systems. *Journal of the Geological Society*, **155**(2):217-222. doi: 10.1144/gsjgs.155.2.0217

Carvajal C.R. & Steel R.J. 2006. Thick turbidite successions from supply-dominated shelves during sea-level highstand. *Geology*, **34**(8):665-668. doi: 10.1130/G22505.1

Catuneanu O. 2006. *Principles of sequence stratigraphy*. Amsterdam, Elsevier, 375p.

Catuneanu O., Abreu V., Bhattacharya J.P., Blum M.D., Dalrymple R.W., Eriksson P.G., Fielding C.R., Fisher W.L., Galloway W.E., Gibling M.R., Giles K.A., Holbrook J.M., Jordan R., Kendall C.G.St.C., Macurda B., Martinsen O.J., Miall A.D., Neal J.E., Nummedal D., Pomar L., Posamentier H.W., Pratt B.R., Sarg J.F., Shanley K.W., Steel R.J., Strasser A., Tucker M.E., Winker C. 2009. Towards the standardization of sequence stratigraphy. *Earth-Science Reviews*, **92**:1-33.

Chang H.K., Assine M.L., Corrêa F.S., Tinen J.S., Vidal A.C., Koike L. 2008. Sistemas petrolíferos e modelos de acumulação de hidrocarbonetos na bacia de Santos. *Revista Brasileira de Geociências*, **38**(2):29-46.

Clausen O.R., Śliwińska K.K., Gołędowski B. 2012. Oligocene climate changes controlling forced regression in the eastern North Sea. *Marine and Petroleum Geology*, **29**:1-14.

D'Ávila R.S.F., Arienti L.M., Aragão M.A.N.F., Vesely F.F., Santos S.F., Voelcker H.E., Viana A.R., Kowsmann R.O., Moreira J.L.P., Coura A.P.P., Paim P.S.G., Matos R.S., Machado L.C.R. 2008. Ambientes de águas profundas. *In*: Silva A.J.C.L.P., Aragão M.A.N.F., Magalhães A.J.C. (Orgs.). *Ambientes de sedimentação siliciclástica do Brasil*. São Paulo, Beca, p. 244-300.

de Gasperi A. & Catuneanu O. 2014. Sequence stratigraphy of the Eocene turbidite reservoirs in Albacora field, Campos Basin, offshore Brazil. *AAPG Bulletin*, **98**(2):279-313. doi: 10.1306/07031312117

Deckers J. 2015. Middle Miocene mass transport deposits in the southern part of the Roer Valley Graben. *Marine and Petroleum Geology*, **66**(4):653-659.

Dias J.L. 2008. Estratigrafia e sedimentação dos evaporitos neo-aptianos na margem leste brasileira. *In*: Mohriak W.U., Szatman P., Anjos S.M.C. (Orgs.). *Sal – geologia e tectônica*. São Paulo, Beca, p. 220-229.

Dixon J.F. 2013. *Shelf-edge deltas: stratigraphic complexity and relationship to deep-water deposition*. PhD Thesis, University of Texas, 217 p.

Dixon J.F., Steel R.J., Olariu C. 2012. Shelf-edge delta regime as a predictor of deep-water deposition. *Journal of Sedimentary Research*, **82**(9):681-687. doi: 10.2110/jsr.2012.59

Dixon J.F., Steel R.J., Olariu C. 2013. A model for cutting and healing of deltaic mouth bars at the shelf edge: mechanism for basin-margin accretion. *Journal of Sedimentary Research*, **83**(3):284-299. doi: 10.2110/jsr.2013.25

Duarte C.S.L. & Viana A.R. 2007. Santos Drift system: stratigraphic organization and implications for late Cenozoic palaeocirculation in the Santos Basin, SW Atlantic Ocean. *In*: Viana A.R. & Rebesco M. (Eds.). *Economic and Palaeoceanographic Significance of Contourite Deposits*, **276**:171-198.

Friedrichs C.T. & Wright L.D. 2004. Gravity-driven sediment transport on the continental shelf: implications for equilibrium profiles near river mouths. *Coastal Engineering*, **51**(8-9):795-811.

Gamboa D., Alves T.M., Cartwright J.A. 2012. Seismic-scale rafted and remnant blocks over salt ridges in the Espírito Santo Basin, Brazil. *In*: Yamada Y., Kawamura K., Ikehara K., Ogawa Y., Urgeles R., Mosher D., Chaytor J., Strasser M. (Eds.). *Submarine mass movements and their consequences*. Berlin, Springer, p. 629-638. doi: 10.1007/978-94-007-2162-3_56

Garcia S.F.M., Letouzey J., Rudkiewicz J.-L., Danderfer Filho A., de Lamotte D.F. 2012. Structural modeling based on sequential restoration of gravitational salt deformation in the Santos Basin. *Marine and Petroleum Geology*, **35**(1):337-353.

Gee M.J.R., Gawthorpe R.L., Bakke K., Friedmann S.J. 2007. Seismic geomorphology and evolution of submarine channels from the Angolan continental margin. *Journal of Sedimentary Research*, **77**(5-6):433-446. doi: 10.2110/jsr.2007.042

Hadler-Jacobsen F., Gardner M.H., Borer J.M. 2007. Seismic stratigraphic and geomorphic analysis of deep-marine deposition along the West African continental margin. *In*: Davies R.J., Posamentier H.W., Wood L.J., Cartwright J.A. (Eds.). Seismic geomorphology: applications to hydrocarbon exploration and production. *Geological Society Special Publication*, **277**:47-84.

Helland-Hansen W. & Hampson G.J. 2009. Trajectory analysis: concepts and applications. *Basin Research*, **21**(5):454-483.

Henriksen S., Helland-Hansen W., Bullimore S. 2010. Relationships between shelf-edge trajectories and sediment dispersal along depositional dip and strike: a different approach to sequence stratigraphy. *Basin Research*, **23**(1):3-21. doi: 10.1111/j.1365-2117.2010.00463.x

Jiang S., Weimer P., Henriksen S., Hammon III W.S. 2012. 3D seismic stratigraphy and evolution of Upper Pleistocene deepwater depositional systems, Alaminos Canyon, northwestern deep Gulf of Mexico. *In*: Prather B.E., Deptuck M.E., Mohrig D., Van Hoorn B., Wynn R.B. *Application of the principles seismic geomorphology to continental-slope and base-of-slope systems:* case studies from seafloor and near-seafloor analogues. Society for Sedimentary Geology (SEPM) Special Publication, **99**:309-327. doi: 10.2110/pec.12.99.0309

Johannessen E.P. & Steel R.J. 2005. Shelf-margin clinoforms and prediction of deepwater sands. *Basin Research*, **17**(4):521-550.

Karner G.D. & Driscoll N.W. 1999. Tectonic and stratigraphic development of the West African and Eastern Brazilian margins: insights from quantitative basin modeling. *In*: Cameron N.R., Bate R.H., Clure V.S. (Eds.). The oil and gas habitats of the South Atlantic. *Geological Society*, **153**:11-40. doi: 10.1144/GSL.SP.1999.153.01.02

Kolla V. & Perlmutter M.A. 1993. Timing of turbidite sedimentation on the Mississippi Fan. *AAPG Bulletin*, **77**(7):1129-1141.

Lourens L.J., Sluijs A., Kroon D., Zachos J.C., Thomas E., Röhl U., Bowles J., Raffi I. 2005. Astronomical pacing of late Palaeocene to early Eocene global warming events. *Nature*, **435**(7045):1083-1087.

Macedo J.M. 1989. Evolução tectônica da bacia de Santos e áreas continentais adjacentes. *Boletim de Geociências da Petrobras*, **3**:159-173.

Machado L.C.R., Kowsmann R.O., Almeida Jr. W., Murakami C.Y., Schreiner S., Miller D.J., Piauilino P.O.V. 2004. Geometria da porção proximal do sistema deposicional turbidítico moderno da Formação Carapebus, bacia de Campos; modelo para heterogeneidades de reservatório. *Boletim de Geociências da Petrobras*, **12**(2):287-315.

Martinez J.F., Cartwright J., Hall B. 2005. 3D seismic interpretation of slump complexes: examples from the continental margin of Israel. *Basin Research*, **17**:83-108. doi: 10.1111/j.1365-2117.2005.00255.x.

Mellere D., Plink-Björklund P., Steel R.J. 2002. Anatomy of shelf deltas at the edge of a prograding Eocene shelf margin, Spitsbergen. *Sedimentology*, **49**(6):1181-1206. doi: 10.1046/j.1365-3091.2002.00484.x.

Mitchum R.M., Vail P.R., Sangree J.B. 1977a. Seismic stratigraphy and global changes in sea level, part 6: stratigraphic interpretation of seismic reflection patterns in depositional sequences. *In:* Payton C.E. (ed.). *Seismic stratigraphy: application to hydrocarbon exploration*, **26**:117-133.

Mitchum R.M., Vail P.R., Thompson S. 1977b. Seismic stratigraphy and global changes in sea level, part 2: the depositional sequence as a basic unit for stratigraphic analysis. *In:* Payton C.E. (Ed.). *Seismic stratigraphy: application to hydrocarbon exploration*, **26**:53-62.

Modica C.J. & Brush E.R. 2004. Postrift sequence stratigraphy, paleogeography, and fill history of the deep-water Santos Basin, offshore southeast Brazil. *AAPG Bulletin*, **88**(7):923-945.

Mohriak W.U. & Magalhães J.M. 1993. Estratigrafia e evolução estrutural da área norte da bacia de Santos. *In*: III Simpósio de Geologia do Sudeste, *Atas*, v. 1, p. 19-26.

Moreira J.L.P. & Carminatti M. 2004. Sistemas deposicionais de talude e bacia no Eoceno da bacia de Santos. *Boletim de Geociências da Petrobras*, **12**(1):73-87.

Moreira J.L.P., Madeira C.V., Gil J.A., Machado M.A.P. 2007. Bacia de Santos. *Boletim de Geociências da Petrobras*, **15**(2):531-549.

Moreira J.L.P., Nalpas T., Joseph P., Guillocheau F. 2001. Stratigraphie sismique de la marge Eocène du Nord du Bassin de Santos (Brésil): relations plateforme/systèmes turbiditiques; distortion des séquences de dépôt. *Comptes Rendus de l'Académie des Sciences, Earth and Planetary Sciences*, **332**(8):491-498.

Moscardelli L., Wood L., Mann P. 2006. Mass-transport complexes and associated processes in the offshore area of Trinidad and Venezuela. *AAPG Bulletin*, **90**(7):1059-1088. doi: 10.1306/02210605052

Muto T. & Steel R.J. 2002. In defense of shelf-edge delta development during falling and lowstand of relative sea level. *The Journal of Geology*, **110**(4):421-436. doi: 10.1086/340631.

Mutti E. & Normark W.R. 1991. An integrated approach to the study of turbidite systems. *In:* Weimer P. & Link M.H. (Eds.). *Seismic facies and sedimentary processes of submarine fans and turbidite systems*. London, Springer, p. 75-106.

Omosanya K.O. & Alves T.M. 2013. A 3-dimensional seismic method to assess the provenance of mass-transport deposits (MTDs) on salt-rich continental slopes (Espírito Santo Basin, SE Brazil). *Marine and Petroleum Geology*, **44**:223-239.

Patruno S., Hampson G.J., Jackson, C.A.-L. 2015. Quantitative characterisation of deltaic and subaqueous clinoforms. *Earth-Science Reviews*, **142**:79-119.

Plink-Björklund P. & Steel R.J. 2002. Sea-level fall below the shelf edge, without basin-floor fans. *Geology*, **30**(2):115-118. doi: 10.1130/0091-7613.

Porębski S.J. & Steel R.J. 2003. Shelf-margin deltas: their stratigraphic significance and relation to deepwater sands. *Earth-Science Reviews*, **62**:283-326.

Posamentier H.W. & Erskine R.D. 1991. Seismic expression and recognition criteria of ancient submarine fans. *In*: Weimer P., Link M.H. (Eds.). *Seismic facies and sedimentary processes of modern and ancient submarine fans and turbidite systems*. Springer, 197-222.

Posamentier H.W. & Kolla V. 2003. Seismic geomorphology and stratigraphy of depositional elements in deep-water settings. *Journal of Sedimentary Research*, **73**(3):367-388. doi: 10.1306/111302730367.

Posamentier H.W., Martinsen O.J. 2011. The character and genesis of submarine mass-transport deposits: insights from outcrop and 3D seismic data. *In*: Shipp R.C., Weimer P., Posamentier H.W. (Eds.). *SEPM Special Publication*, **96**:7-38.

Posamentier H.W., Davies R.J., Cartwright J.A., Wood L.J. 2007. Seismic geomorphology – an overview. *In*: Davies R.J., Posamentier H.W., Wood L.J., Cartwright J.A. (Eds.). *Seismic geomorphology: applications to hydrocarbon exploration and production*, Special Publication, p. 1-14.

Prather B.E. & Steele D.R. 2000. Methodologies for uncertainty assessment of deep-water facies and basins. *In*: Appi C.J. (Ed.). *Deep-water sedimentation: technological challenges for the next millennium – 31st International Geological Congress*. Rio de Janeiro, ABGP, p. 85-92.

Prather B.E., Deptuck M.E., Mohrig D., van Hoom B., Wynn R.B. 2012. Application of the principles of seismic geomorphology to continental-slope and base-of-slope systems: case studies from seafloor and near-seafloor analogues. *In*: Prather B.E., Deptuck M.E., Mohrig D., Van Hoorn B., Wynn R.B. *Application of the principles seismic geomorphology to continental slope and base-of-slope systems:* case studies from seafloor and near-seafloor analogues, Special Publication, **99**:5-9. doi: 10.2110 /pec.12.99.0005.

Ribeiro M.C.S. 2007. *Termocronologia e história denudacional da Serra do Mar e implicações no controle deposicional da bacia de Santos*. PhD Thesis, Instituto de Geociências e Ciências Exatas, Universidade Estadual Paulista, Rio Claro, 227 p.

Safronova P.A., Henriksen S., Andreassen K., Laberg J.S., Vorren T.O. 2014. Evolution of shelf-margin clinoforms and deep-water fans during the middle Eocene in the Sørvestsnaget Basin, southwest Barents Sea. *AAPG Bulletin*, **98**(3):515-544.

Sahy D., Condon D.J., Terry Jr. D.O., Fischer A.U., Kuiper K.F. 2015. Synchronizing terrestrial and marine records of environmental change across the Eocene-Oligocene transition. *Earth and Planetary Science Letters*, **427**:171-182. doi: 10.1016/j.epsl.2015.06.057.

Saller A. & Dharmasamadhi I.N.W. 2012. Controls on the development of valleys, canyons, and unconfined channel-levee complexes on the Pleistocene slope of East Kalimantan, Indonesia. *Marine and Petroleum Geology*, **29**:15-34.

Shanmugam G. 2000. 50 years of the turbidite paradigm (1950s – 1990s): deep-water processes and facies models – a critical perspective. *Marine and Petroleum Geology*, **17**(2):285-342.

Shanmugam G. 2002. Ten turbidite myths. *Earth-Science Reviews*, **58**:311-341.

Sombra C.L., Arienti L.M., Pereira M.J., Macedo J.M. 1990. Parâmetros controladores da porosidade e da permeabilidade nos reservatórios clásticos profundos do Campo de Merluza, bacia de Santos, Brasil. *Boletim de Geociências da Petrobras*, **4**(4):451-466.

Steel R.J. & Olsen T. 2002. Clinoforms, clinoform trajectories and deepwater sands. *In*: Armentrout J.M. & Rosen N.C. (Eds.). *Sequence stratigraphic models for exploration and production: evolving models and application histories*, GCS-SEPM Special Publication, **22**:367-381.

Stow D.A.V. & Mayall M. 2000. Deep-water sedimentary systems: new models for the 21st century. *Marine and Petroleum Geology*, **17**(2):125-135. doi:10.1016/S0264-8172(99)00064-1.

Sydow J., Roberts H.H., Bouma A.H., Winn, R. 1992. Constructional subcomponents of shelf-edge delta, northeast Gulf of Mexico. *Gulf Coast Association of the Geological Societies Transactions*, **42**:717-726.

Sylvester Z., Deptuck, M.E., Prather B.E., Pirmez C., O'Byrne C. 2012. Seismic stratigraphy of a shelf-edge delta and linked submarine channels in the northeastern Gulf of Mexico. *In*: Prather B.E., Deptuck M.E., Mohrig D., van Hoorn B., Wynn R.B. Application *of the principles seismic geomorphology to continental slope and base-of-slope systems:* case studies from seafloor and near-seafloor analogues. Society for Sedimentary Geology (SEPM) Special Publication, **99**:31-59. doi: 10.2110/pec.12.99.0031.

Veeken P.C.H. & Van Moerkerken B. 2013. *Seismic stratigraphy and depositional facies models*. Houten, EAGE, 496 p.

Weimer P. 1989. Sequence stratigraphy of the Mississippi Fan (Plio-Pleistocene), Gulf of Mexico. *Geo-Marine Letters*, **9**:185-272.

Williams B.G. & Hubbard R.J. 1984. Seismic stratigraphic framework and depositional sequences in the Santos Basin. *Marine and Petroleum Geology*, **1**:90-104.

Zalán P.V. & Oliveira J.A.B. 2005. Origem e evolução estrutural do sistema de riftes cenozóicos do Sudeste do Brasil. *Boletim de Geociências da Petrobras*, **13**(2):269-300.

Zecchin M. & Catuneanu O. 2013. High-resolution sequence stratigraphy of clastic shelves I: units and bounding surfaces. *Marine and Petroleum Geology*, **39:**1-25.